Isothermal Crystallization Kinetics of Anhydrous Sodium Acetate Nucleated Poly(Ethylene Terephthalate)

V. D. Deshpande, Sandeep Jape

Department of Physics, Institute of Chemical Technology, Mumbai, India

Received 15 July 2009; accepted 28 November 2009
DOI 10.1002/app.31891
Published online 22 February 2010 in Wiley InterScience (www.interscience.wiley.com).

ABSTRACT: Studies on the isothermal crystallization kinetics of poly(ethylene terephthalate) (PET) nucleated with anhydrous sodium acetate were carried out. The nucleated agent had succeeded in promoting greater rates of crystallization in PET. A study of the melting behavior of the samples revealed that the nucleating agents promoted formation of thinner lamellae. The equilibrium melting temperature (T_m^0) of samples was determined using linear and nonlinear Hoffman Weeks procedure. The nonlinear Hoffman Week's procedure was found to be inapplicable in the current study. The Lauritzen-Hoffman secondary nucleation theory was applied to determine the nucleation parameter (K_g), fold surface energy (σ_e), and work of chain folding (q). σ_e and q decreased on addition of nucleating agent. The approximate and exact form of the Lauritzen Z-test was used to determine the operating regime. The operating regime was found to be primarily regime II for the range of temperatures studied. © 2010 Wiley Periodicals, Inc. J Appl Polym Sci 116: 3541–3554, 2010

Key words: crystallization; differential scanning calorimetry; kinetics (polym.); melt; polyesters

INTRODUCTION

The crystallization kinetics of nucleated poly(ethylene terephthalate) (PET) has been the subject of several studies.[1–16] The additives include inorganic compounds such as talc [$Mg_3Si_4O_{10}(OH)_2$], $CaSO_4$, $CaCO_3$, SiO_2, TiO_2, $A1_2O_3$, $BaSO_4$, CaO, MgO;[1–3] metal hydroxide like $Al(OH)_3$;[4] halogenated salts as KCl;[5] trimethylphosphate [$(CH_3)_3PO_4$] and calcium acetate ($C_4H_6O_4Ca$)[6] as well as sodium salts.[7–10] The term "chemical nucleation" was used to describe the mechanism of a class of agents involving sodium salts.[11–15] These agents differed from conventional particle nucleants in regards to the mechanism with which they promoted the formation of primary nuclei. These agents when added to polyesters tended to react with it creating products that would eventually acted as sites for formation of the primary nuclei. In a previous nonisothermal study conducted by us,[16] we had demonstrated that sodium acetate (SA) acted as a chemical nucleant. The agent had succeeded in increasing the overall rates of crystallization by creation of sodium terephthalate chain ends through chain scission of PET. The combined effect of decreased molecular weight and an increase in the number of available sites contributed in promoting greater crystallization rates in PET. However, the continuous rise in the bulk crystallization rates was observed only for low concentrations. At higher concentrations, the unreacted SA by agglomerating caused a decrease in the nucleation as well as the overall crystallization rates. The present work aims to study effect of addition of SA to PET under isothermal conditions.

Crystallization kinetics

The Avrami equation is generally used to describe the isothermal crystallization behavior in polymers. The Avrami equation is of the form:[17–19]

$$1 - X(t) = \exp(-kt^n), \tag{1}$$

where $X(t)$ is the relative crystallinity as a function of time and the parameter k is the rate constant, n is Avrami exponent which depends on the type of nucleation and the growth dimension.

The relative crystallinity $X(t)$ at time t can be calculated from the equation:

$$X(t) = \int_0^t (dH/dt)dt \Big/ \int_0^\infty (dH/dt)dt, \tag{2}$$

where $t = 0$ is the start time and $t = \infty$ is the end time of the crystallization curve. In eq. (2), the

Correspondence to: V. D. Deshpande (vindesh2@rediffmail.com).

Contract grant sponsor: University Grants Commission, Government of India, New Delhi [under Special Assistance Program (SAP)]; contract grant number: F.4-1/2006(BSR)/5-65/2007.

numerator corresponds to the area under the crystallization curve up to time t; the denominator is the total area in the crystallization curve.

Taking double logarithms, eq. (1) can be expressed in the following form:

$$\log[-\ln\{1 - X(t)\}] = n \log t + \log k. \quad (3)$$

Plotting the first term log [–ln {1–X (t)}] as a function of log t, the Avrami parameters, n (slope) and k (intercept) can be obtained.

Surface nucleation theory

The process of crystallization involves nucleation and growth. The growth of the initially formed primary nuclei is often described by the secondary nucleation theory developed by Hoffman and Lauritzen. According to this theory, the spherulite growth rate (G) can be expressed in the form[20]:

$$G = G_0 \exp\left(-\frac{U^*}{R(T_c - T_\infty)}\right) \exp\left(\frac{K_g}{T_c(\Delta T)f}\right), \quad (4)$$

where G_0 is a temperature independent pre-exponential term, U^* is transport activation energy of polymer segments to the liquid crystal interface, and R is the gas constant. $\Delta T = (T_m^0 - T_c)$ is the undercooling, where T_m^0 is the equilibrium melting temperature and T_c is the crystallization temperature. T_∞ is the temperature below which viscous flow ceases, usually given by $T_\infty = T_g - 30$ K. $f = 2T_c/(T_c + T_m^0)$ which is the correction factor to account for the change in enthalpy of fusion with temperature. K_g is the nucleation parameter given by the following equation:

$$K_g = \frac{mb\sigma\sigma_e T_m^0}{k_B \Delta H_f}, \quad (5)$$

where m is the regime parameter; it has a value of four for regime I and two for regime II. b is the monomolecular layer thickness corresponding to the perpendicular distance between the (010) planes and is taken to be 5.53Å.[21] ΔH_f is the enthalpy of fusion per unit volume (2.1×10^8 J/m^3)[22] and k_B is the Boltzman constant (1.35×10^{-23} J/K). The parameters σand σ_e are the lateral and fold surface free energies respectively. Regime I is characterized by a process where a single surface nucleus causes completion of substrate of length L, where it corresponds to distance between chain defects. The overall growth rate is then proportional to the nucleation rate i. Spherulitic growth occurs though addition of layer of substrate of thickness b and is given by $G = biL$. In regime II, which occurs at lower undercooling, multiple surface nucleating acts occur on the substrate at a rate comparable with substrate completion rate (g) so that G is given by $G = b(2ig)^{1/2}$.

EXPERIMENTAL

Sample preparation

PET was provided by the PET division of Reliance Industries (Patalganga, India). SA was obtained from S.D. Fine Chemicals (Mumbai, India). The polymer and the salt were dried at 110°C for 4 h before blending. The blending was carried out in a Haake Minilab (Thermo Electron, Karlsruhe, Germany) at 280°C and 80 rpm. The polymer was mixed for 5 min before the salt was added. The salt was added to the polymer melt. The samples, 5 min after the addition of the salt, were extruded and quenched in cold water. The quenched samples were then reheated at 75°C for 4 h to remove any trapped water.

Differential scanning calorimetry studies

The crystallization studies were carried out with a PerkinElmer (Waltham, MA) differential scanning calorimetry (DSC)-7 instrument operating under a nitrogen atmosphere of 0.5 kg/cm^2. Throughout the experiment, the sample weight was kept constant at 7 mg. The instrument was calibrated with an indium standard. The crystallization studies were carried out for pure PET and PET nucleated with 1, 3, 5, and 10 wt % SA. The samples were heated from 50 to 300°C at 10°C/min where they were held for 5 min to ensure complete melting. They were then cooled back to desired isothermal temperature at the rate of 160°C/min where it was held for 60 min. The isothermal temperatures (T_c) selected were 195°C, 200°C, 205°C, 210°C, 215°C, 220°C, 225°C, and 230°C.

RESULTS AND DISCUSSION

Avrami analysis

Figure 1(a,b) shows crystallization isotherms of pure and nucleated PET. As T_c is decreased, the curves tend to be narrower. Also, in the nucleated samples, at lower T_c, there was difficulty in assigning the starting point of the isotherm due to incomplete thermal equilibrium achieved. Figure 2(a) displays a typical plot of relative crystallinity versus time. The curves move towards a shorter time scale with decreasing temperature. Since the Avrami equation is used to describe free growth till impingement only the linear portion of the graph corresponding to 5–80% conversion was used for the Avrami plots. The Avrami parameters, k and n, obtained from Avrami plots such as Figure 2(b), as well as $t_{0.5}$ that

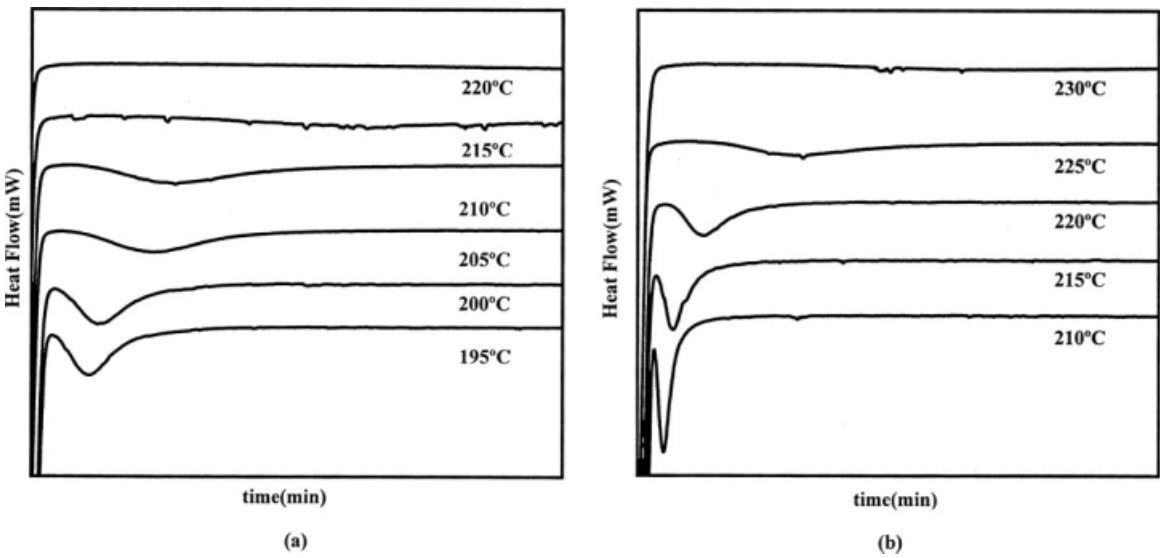

Figure 1 Representative isotherms of (a) pure PET (b) PET +10% SA for different isothermal temperatures.

is the time taken for 50% conversion are displayed in Figure 3 and Table I. For a particular sample, k increases with a decrease in the isothermal temperature. This crystallization behavior is typically observed in a nucleation controlled temperature region. For a particular isothermal temperature, k continuously increases with addition of nucleating agent. Thus, the addition of SA has succeeded in promoting greater rates of crystallization in PET. This is also reflected in the values of $t_{0.5,}$ which decrease as the concentration of SA increases. The induction time (τ_i), that is, the time taken for 5% conversion[23] can be considered to be the time taken for the primary nuclei to form. Figure 4 shows the induction time (τ_i)of the samples. τ_i reduces as the concentration of SA increases. The exponent, n, which initially tends to increase at lower concentrations, decreases at higher concentrations of SA. A similar behavior was seen during nonisothermal crystallization.[16] n ranges between two and three; however it remains closer to three. This corresponds to three dimensional growth with athermal nucleation. Higher n values at lower concentrations can be attributed either to some morphological change or to the nucleation being more sporadic. Chisholm and Zimmer,[24] for PET nucleated with sodium salts, found a similar increase in the Avrami exponent. They authors had attributed it to the sporadic formation of nuclei. For a particular sample, the exponent tended to show a weak decreasing trend with a decrease in temperature. This can be attributed to the fact that at a larger undercoolings an increasing number of primary nuclei, smaller in size, are athermally generated.[25] The free energy barrier to the

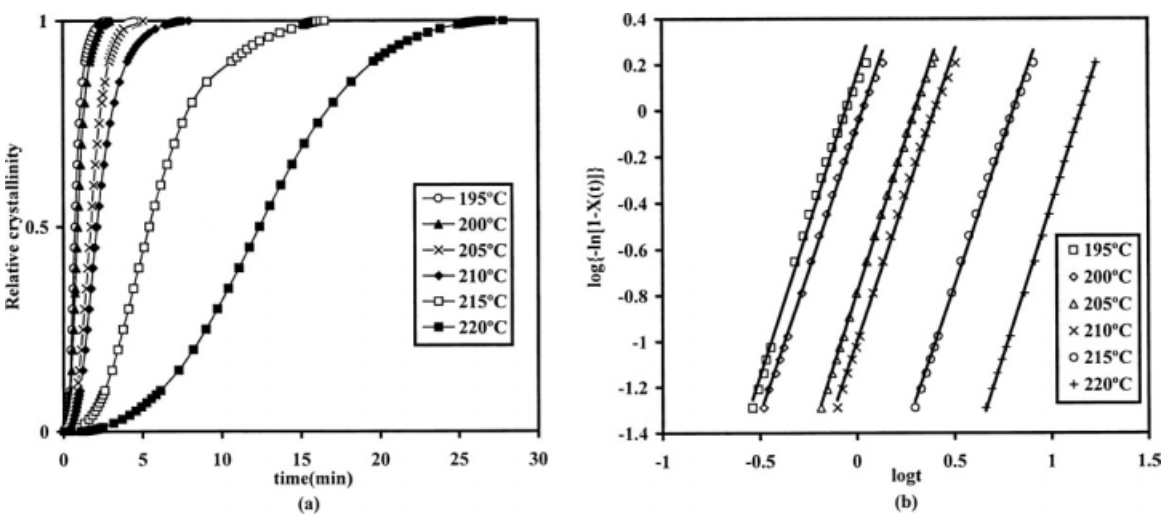

Figure 2 Representative plots of (a) relative crystallinity vs. time (b) Avrami plots, for pure PET at different isothermal temperatures.

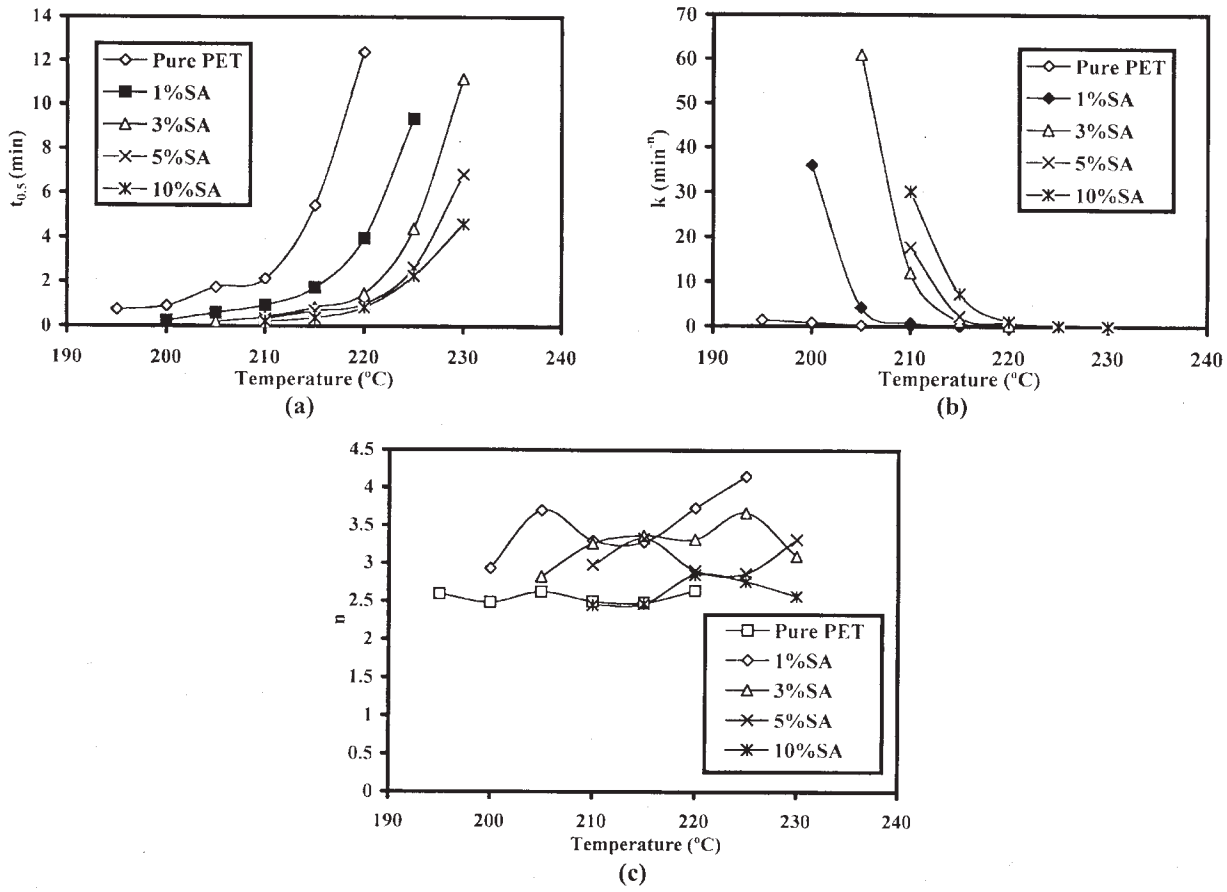

Figure 3 Variation of (a) halftime ($t_{0.5}$) (b) Avrami rate constant (k) (c) Avrami exponent (n) with wt % SA.

formation of critical nucleus has an inverse undercooling dependence. At larger undercooling, the free energy barrier is further lowered for a nucleus formed on a heterogeneous impurity. This can cause a large number of nuclei to form instantaneously thereby contributing to the lowering of n values in the nucleated samples. At smaller undercooling (higher free energy barrier), due to greater chain mobility there can be a greater disruption to formation of critical nuclei. This can cause the nuclei (larger in size) to form sporadically. At higher concentrations, 5–10%, for lower isothermal temperatures, 210–215°C, an incomplete equilibrium formed can lead to error in the observed values of $t_{0.5}$ as well as the Avrami parameters.[26,27] However, despite this, it can be surmised that the overall crystallization rate has shown a continuous increase with concentration of SA. The addition of SA to PET through creation of the sodium terephthalate chain ends has made available a number of sites for heterogeneous nucleation. This has resulted in an increase in primary nucleation rates, with SA content, which is reflected in reduction in τ_i. The higher nucleation rates contribute to the increase in the overall bulk crystallization rates in the samples. These results, however, are inconsistent with the trend obtained during nonisothermal crystallization. During nonisothermal crystallization, an increase in nucleation and overall crystallization rates was obtained only unto 1% SA, decreasing for higher concentrations. In a nonisothermal process, the cooling rate plays an important role in crystallization process. Under these conditions, especially for higher concentrations, there is a greater scope for nucleation process being affected. This may account for the reported decrease in nucleation rates.

Melting behavior

The samples, after isothermal crystallization, were heated at 10°C/min to obtain the corresponding melting endotherms. Figure 5(a) shows the observed melting endotherms for pure PET. Figures 5(b–e) displays the melting behavior of nucleated PET. The observed melting behavior has revealed the presence of three peaks in all samples whose position and intensity depended on the isothermal crystallization temperature. All the samples exhibited similar melting behavior. The melting behavior of pure PET has been studied extensively.[22,28–30] Peak I is usually attributed due to the melting of small lamellar crystals formed during secondary crystallization.[22,28]

TABLE I
Avrami Parameters and Halftime of Crystallization of Samples

Sample	Temperature (°C)	k (min^{-n})	n	$t_{0.5}$ (minutes)	r^2
Pure PET	195	1.39	2.60	0.75	0.9955
	200	8.33×10^{-1}	2.48	0.91	0.9988
	205	1.62×10^{-1}	2.62	1.75	0.9993
	210	9.97×10^{-2}	2.50	2.13	0.9971
	215	9.99×10^{-3}	2.48	5.43	0.9976
	220	8.95×10^{-4}	2.64	12.38	0.9996
1% SA	200	3.60×10^{1}	2.93	0.25	0.9932
	205	4.18	3.70	0.6	0.989
	210	7.48×10^{-1}	3.30	0.95	0.9931
	215	9.87×10^{-2}	3.28	1.74	0.9876
	220	3.69×10^{-3}	3.73	3.95	0.9932
	225	6.14×10^{-5}	4.16	9.35	0.9979
3% SA	205	6.09×10^{1}	2.82	0.2	0.9967
	210	1.20×10^{1}	3.26	0.41	0.9962
	215	1.13	3.37	0.85	0.9967
	220	1.78×10^{-1}	3.32	1.47	0.9956
	225	2.20×10^{-3}	3.67	4.39	0.9963
	230	4.84×10^{-3}	3.09	11.17	0.9957
5% SA	210	1.76×10^{1}	2.98	0.33	0.9986
	215	2.29	3.33	0.69	0.9982
	220	6.84×10^{-1}	2.91	1	0.9997
	225	3.98×10^{-2}	2.87	2.63	0.9957
	230	1.16×10^{-3}	3.31	6.84	0.9999
10% SA	210	3.07×10^{1}	2.45	0.21	0.9908
	215	7.23	2.47	0.38	0.9951
	220	1.07	2.85	0.84	0.9944
	225	6.80×10^{-2}	2.76	2.26	0.9958
	230	1.34×10^{-2}	2.57	4.6	0.9979

These crystallites are formed between the stacks of primary lamellae.[29] Peak II is a result of melting of primary crystallites formed at isothermal crystallization temperature. Peak III is due to melting of crystals that have perfected as result of recrystallization during heating.[22,28,29] The recrystallization process involves reordering of exiting lamellae. According to Hay and coworker[28] such a process would also involve incorporation of amorphous material formed as a result melting of secondary lamellar crystals onto existing primary lamellae. It should be noted that peak III, for isothermal temperatures 215°C and higher, remain absent for all concentrations. This indicates that the higher temperatures are not favorable to recrystallization. At higher crystallization temperature, the lamellae would tend to be more ordered and hence there would be lesser opportunity for ordering through recrystallization.[31] Peak I increases in size with an increase in the isothermal temperature and tends to merge with the peak II appearing as a bump on the lower temperature side. Peak I and II both shifts to higher temperature with increasing isothermal temperature indicating an increase in the corresponding lamellar thickness. For a particular sample, peak III, apart from a decrease in area at higher temperatures, did not show much variation in position with T_c. This indicates that it is due to melting of lamellae not formed at the crystallization temperature.[28] Tiganis et al.[31] suggest that crystals that have undergone recrystallization may form same degree of order. This would account for the limited variation of third melting peak with isothermal temperature. The first and second melting peak temperatures tend to decrease with SA concentration indicating that the corresponding lamellar thickness decreases. The third meting peak tended to decrease slightly with SA concentration. This may be a result of lower level of reorganization in those samples. Figure 6 displays the variations of the peak temperatures with wt % SA.

Table II gives the combined melting enthalpy (ΔH_m) of three peaks. ΔH_m can be considered to be a measure of the degree of crystallinity. The degree of crystallinity of the sample can be obtained by dividing the observed melting enthalpy with the melting enthalpy of 100% crystalline material, that is, 120 J/g,[27] for PET. ΔH_m tended to increase slightly at lower temperatures. This may be primarily attributed to increase in the spherulite density although lamellar thickness tends to decrease with decreasing temperature. Furthermore, for a particular temperature, ΔH_m tended to increase with SA only up to 3% SA. At higher concentrations, the melting enthalpy tends to decrease. This indicates that, highest levels of crystallinity are achieved for lower concentrations of SA (up to 3% SA). At the higher concentrations despite the increased crystallization rates, their overall level of crystallinity has decreased slightly. At higher concentrations, the unreacted SA particles like conventional nucleants,[2] may tend agglomerate isolating crystallizable amorphous regions between them. This would lead to the observed overall

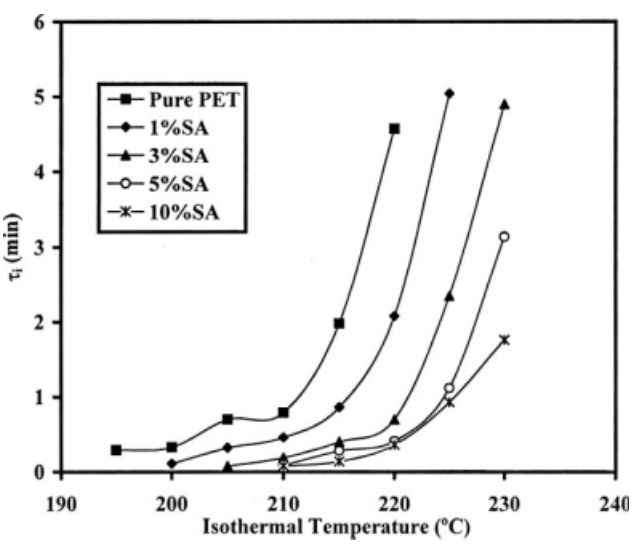

Figure 4 Induction time (τ_i)of pure and nucleated PET at different isothermal temperatures.

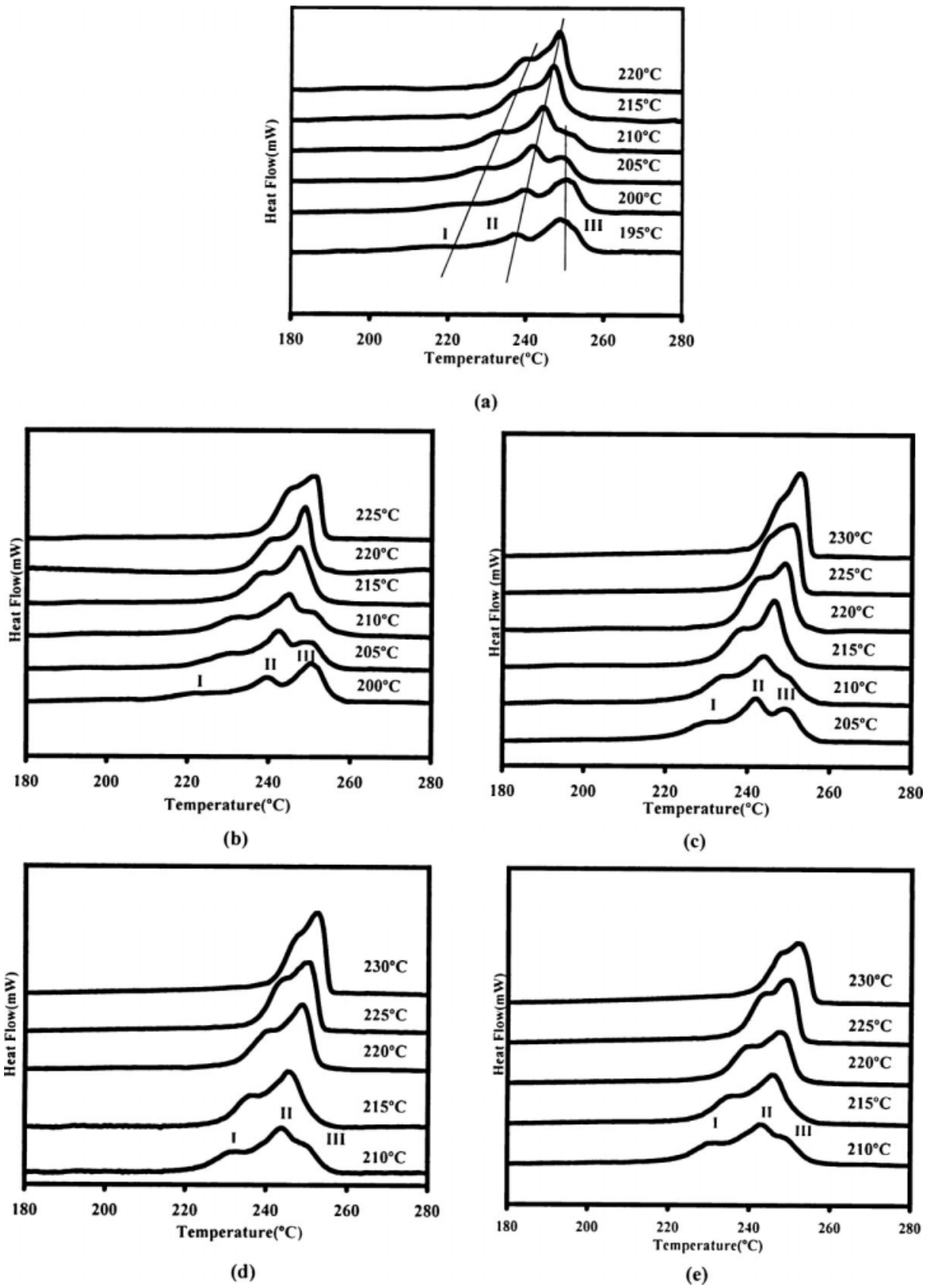

Figure 5 Multiple melting behavior of (a) pure PET (b) 1% SA (c) 3% SA (d) 5% SA (e) 10% SA.

decrease in crystallinity. It should also be noted that, for isothermal temperatures 215°C and below, the melting of the peak formed due to recrystallization contributes towards the overall melting enthalpy. Hence, the observed enthalpy at those temperatures cannot be considered to be the true measure of the

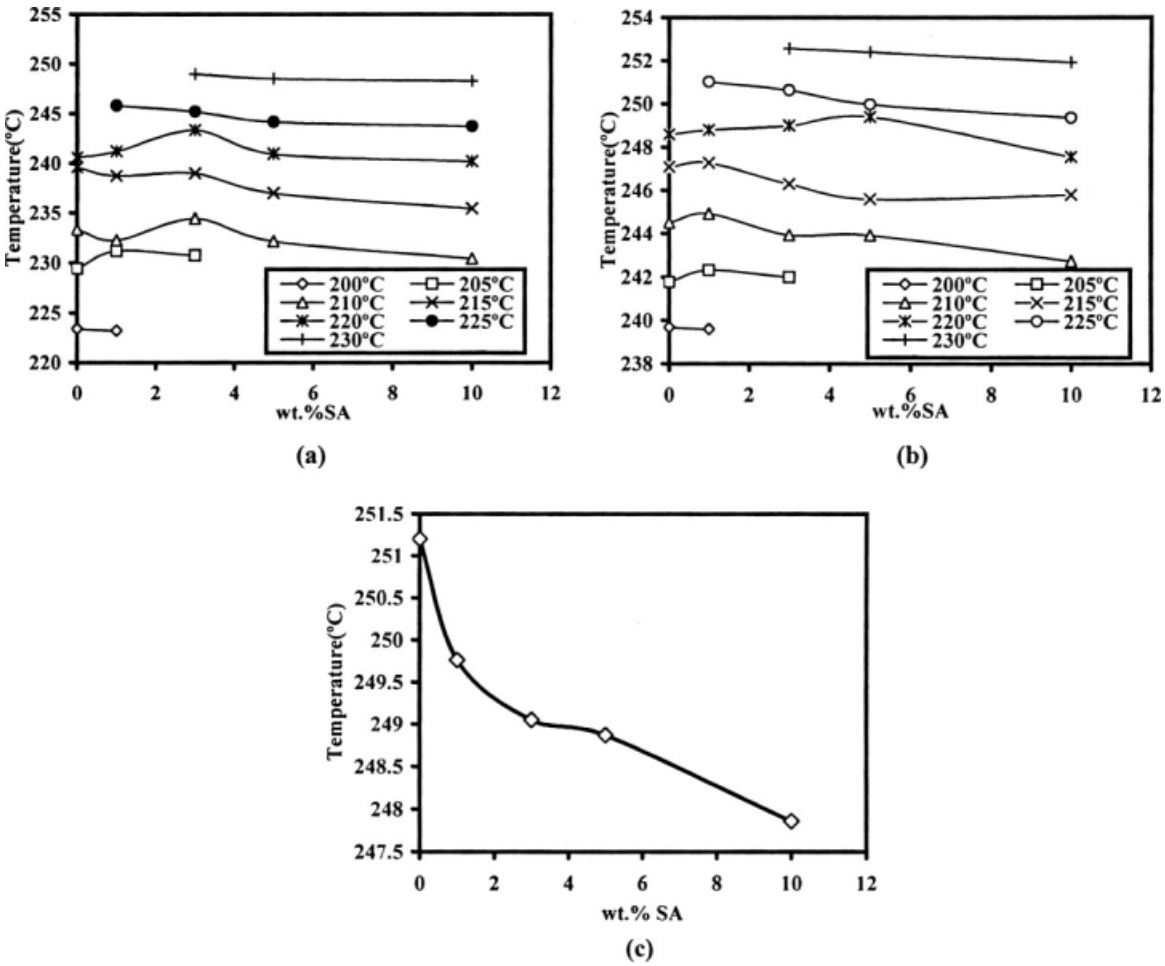

Figure 6 Variation of (a) 1st and (b) 2nd (c) 3rd (for isothermal temperature 210°C) melting peak with wt % SA.

initial level of crystallinity of the samples. The addition of such chemical nucleants at low concentrations, in PET, might result in improved mechanical properties due to an increase in crystallinity. However, any such gains can be nullified by the molecular weight degradation brought about by the nucleating mechanism. Hence, as pointed out by Garcia,[12] the usage in terms of concentration of such nucleants, should be carefully controlled to optimize the desired mechanical properties. Another option would be to add agents such as tetraphenyl borate salts to offset the molecular weight degradation.[32] Further detailed studies would be required to reveal the effect of addition of SA of the mechanical properties of PET.

Equilibrium melting temperature

Linear Hoffman–Weeks extrapolation

It is important to calculate the equilibrium melting temperature to measure the undercooling ($\Delta T = T_m^0 - T_c$). The Hoffman Weeks plot, based on the observed linear relation between melting temperature, T_m and T_c, is often used to determine T_m^0. It is expressed mathematically by the following equation:[33]

$$T_m = \frac{T_c}{2\beta} + T_m^0\left[1 - \frac{1}{2\beta}\right]. \quad (6)$$

The intersection point of the linear extrapolation of T_m versus T_c line with the $T_m = T_c$ line would yield T_m^0. The term β represents the thickening factor, that is ratio of the thickness of final lamellar thickness (l) to the initial lamellar thickness (l^*). The linear Hoffman–Weeks (LHW) plots for pure PET are shown in Figure 7. In the case of the observed multiple melting endotherms, the peak temperature corresponding to the melting of primary crystallites, that is peak II was used for extrapolation. Table III displays the values of the equilibrium melting temperature as well as the thickening factor β for all the samples. The observed values of T_m^0 for pure PET (273.76°C) is close to the value (274°C) obtained elsewhere.[34] The lowering of T_m^0 indicates that addition of SA has resulted in the formation of thinner lamellae in the nucleated samples as compared to pure

TABLE II
Melting Enthalpy and Degree of Crystallinity of Samples

Sample	Temperature (°C)	ΔH_m (J/g) (combined)	% Crystallinity
Pure PET	195	48.196	40.16
	200	54.196	45.16
	205	51.58	42.98
	210	52.758	43.97
	215	51.205	42.67
	220	51.635	43.03
1% SA	200	51.596	46.93
	205	53.878	44.90
	210	52.489	43.74
	215	53.534	44.61
	220	53.212	44.34
	225	50.121	41.77
3% SA	205	54.535	45.45
	210	54.665	45.55
	215	53.122	44.27
	220	53.834	44.86
	225	50.418	42.02
	230	49.061	40.88
5% SA	210	52.189	43.49
	215	52.845	44.04
	220	51.389	42.82
	225	48.163	40.14
	230	48.195	40.16
10% SA	210	45.809	38.17
	215	44.922	37.44
	220	43.797	36.50
	225	42.196	35.16
	230	37.665	31.39

PET. β remained greater than unity in all the samples indicating that lamellar thickening had occurred during isothermal crystallization. The values obtained are higher for all the nucleated samples. This would indicate that, in nucleated samples, the initially formed lamellae tend to attain stability through a greater degree of thickening as compared to pure PET.

NonLinear Hoffman–Weeks extrapolation

The initial lamellar thickness can be expressed in terms of the undercooling through the relation:[20]

$$l^* = \frac{2\sigma_e T_m^0}{\Delta H_f(\Delta T)} + \delta l, \tag{7}$$

where δl is necessary to prevent the lamellae from melting at its crystallization temperature. ΔH_f is the heat of fusion per unit volume and σ_e is the fold surface free energy. Equation (7) in general can be expressed as:[35]

$$l^* = C_1/\Delta T + C_2, \tag{8}$$

where C_1 has a value of $2\sigma_e T_m^0/\Delta H_f$. The term C_2 is a constant which accounts the term δl and the temperature dependence of the kinetic fold surface free energy. The kinetic fold energy arises from fold length protrusion and the mixing entropy associated with stems of different length.[35,36]The contribution of C_2 is ignored in LHW extrapolation. Marand et al.[35] suggested that the contribution of the term C_2 leads to a nonlinear relationship between the observed T_m and T_c. It's neglection can lead to an overestimation of β and an underestimation of T_m^0. In a particular case where the interfacial energy of the plane formed by initial crystals is equal to that formed by mature crystals the following relation was proposed:[35]

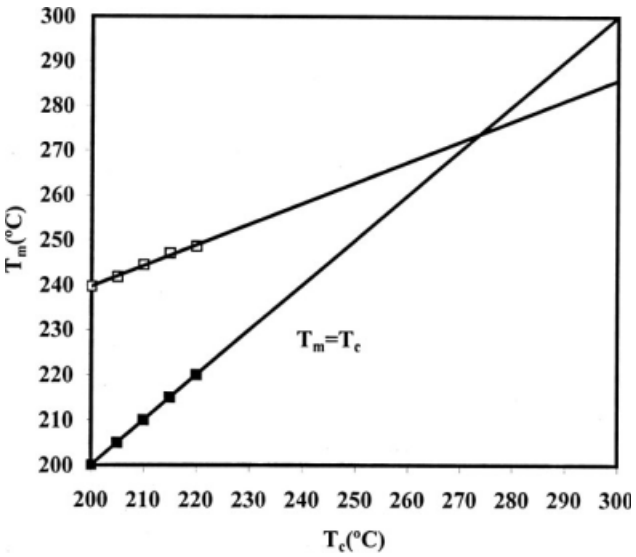

Figure 7 Hoffman Weeks plot for pure PET.

$$M = \beta(X + a), \tag{9}$$

$$M = T_m^0/T_m^0 - T_m, X = T_m^0/T_m^0 - T_c \quad a = C_2\Delta H_f/2\sigma_e.$$

In eq. (9), when M is plotted against X for various values of the T_m^0 (arbitrarily chosen), it would yield different values of the thickening factor β from the slope. The value of T_m^0 for which the plot yields a slope of unity would correspond to the melting temperature of the initial crystals. The T_m^0 values obtained are listed in Table IV. The calculated T_m^0

TABLE III
Equilibrium Melting Temperature and Thickening Coefficient of Samples from Linear Hoffman–Week's Procedure

Sample	T_m^0 (°C)	r^2	β
Pure PET	273.76	0.9956	1.084
1% SA	272.14	0.9944	1.128
3% SA	270.16	0.9924	1.154
5% SA	270.36	0.9871	1.149
10% SA	269.02	0.9901	1.137

TABLE IV
Equilibrium Melting Temperature from Nonlinear Hoffman–Week's Procedure

Sample	T_m^0 (°C)	a	r^2
Pure PET	317.47	1.3806	0.9929
1% SA	309.81	1.6402	0.9906
3% SA	303.16	1.886	0.9919
5% SA	302.45	1.9035	0.9893
10% SA	300.41	1.9289	0.9897

for pure PET from this procedure is lower than the value (323.5°C) obtained by Supaphol and coworkers.[37] The calculated values of T_m^0 from this procedure also show a similar decrease with SA content. There have been few studies[38–42] where the equilibrium melting temperature was determined through the NLHW procedure. The authors, in those cases, had reported a wide difference in the values obtained from LHW and nonlinear Hoffman–Weeks (NHLW) procedures. In the current study, a similar trend is observed. The correlation factor (r^2) for most samples including pure PET is lesser than that obtained from the linear method. This is in contradiction to higher nonlinear r^2 value reported by Supaphol and coworkers.[37] This may be a result of different temperature range selected, that is the current studies were conducted at a higher temperature range. It would be interesting to note the effect of such high value of T_m^0 on different parameters calculated on application of Lauritzen–Hoffman theory to be discussed ahead.

Lauritzen–Hoffman analysis

Equation 5 can be expressed in terms of $t_{0.5}$ through a relation proposed by Chan and Isayev:[43]

$$\left(\frac{1}{t_{0.5}}\right) = \left(\frac{1}{t_{0.5}}\right)_0 \exp\left(-\frac{U^*}{R(T_c - T_\infty)}\right) \exp\left(-\frac{K_g}{T_c(\Delta T)f}\right), \quad (10)$$

where $(1/t_{0.5})_0$ is a temperature independent pre-exponential factor. The values of T_m^0 listed in Tables III and IV were used to calculate ΔT. The other constants include T_g (74°C)—observed from DSC, the gas constant R (8.3144 J/mol/K) and U* (6284 J/mol).[21]

The Hoffman plots calculated using T_{mLHW}^0 are displayed in Figure 8(a). Liu and Hay[22] reported a regime I to regime II transition at the 217°C. While Rahman and Nandi[44] reported a regime I to regime II transition at 236°C, Phillips and Tseng[45] reported a regime II to III transition at 167°C. However, no transition is evident for either pure PET or the nucleated samples, that is, the Hoffman plots using T_{mLHW}^0 remain mostly linear.

The Hoffman plots using T_{mNLHW}^0, shown in Figure 8(b), were similarly obtained. Li and coworkers,[42] or pure polyphylene sulphide (PPS), reported that the T_m^0 value obtained from the nonlinear method better described the regime behavior in terms of ratio of slopes for regimes being same as that theoretically predicted. Marand and coworkers[41] had made a similar conclusion for isotactic polystyrene. In the present case, there appears to be no significant change in the shape of the Hoffman plots. The values of K_g (Table V), obtained from the slope of the Hoffman plots, generally decreased with the addition of SA. The lateral surface energy (σ) can be estimated from the following relation[22]:

$$\sigma = \alpha \Delta H_f (ab)^{1/2}. \quad (11)$$

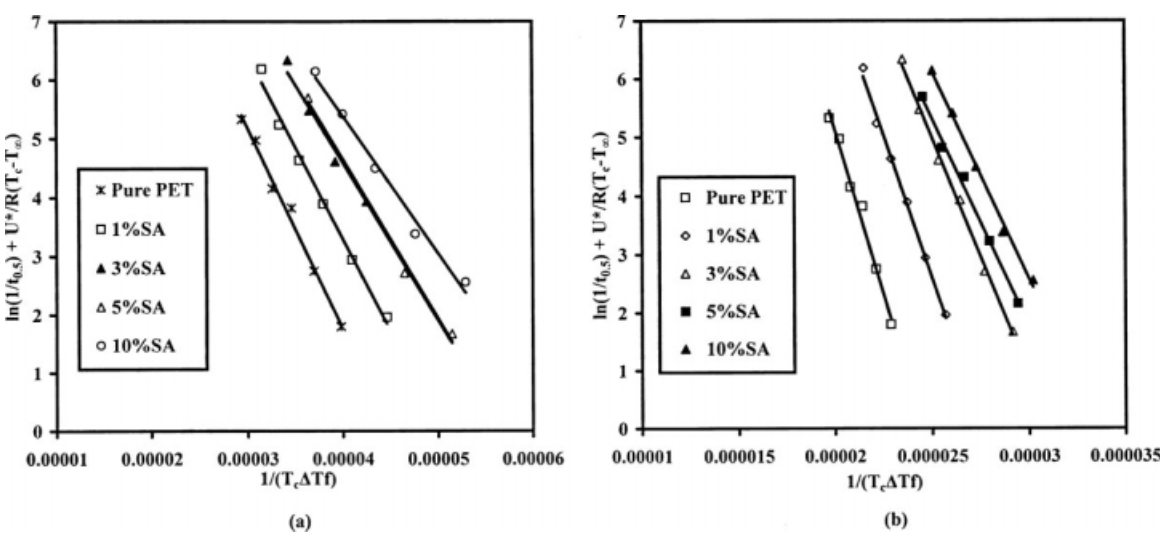

Figure 8 Lauritzen–Hoffman plots for pure and nucleated PET (a) using T_{mLHW}^0 (b) using T_{mNLHW}^0.

TABLE V
Nucleation Parameter Calculated from T^0_{mLHW} and T^0_{mNLHW}

	Nonlinear method		Linear method	
Sample	K_g (K^2)	r^2	K_g (K^2)	r^2
Pure PET	1.129×10^6	0.987	3.424×10^5	0.9908
1% SA	9.763×10^5	0.9958	3.136×10^5	0.9913
3% SA	8.168×10^5	0.9968	2.680×10^5	0.9917
5% SA	7.110×10^5	0.9937	2.344×10^5	0.9938
10% SA	7.106×10^5	0.9945	2.329×10^5	0.9875

In eq. (11) α was taken to be 0.11. It is empirically derived in analogy with behavior of hydrocarbons; a (4.56 Å) and b (5.53 Å) are the monomolecular width and thickness, respectively.[20,21]

The lateral fold surface energy can be used to determine σ_e though substitution in eq. (5). σ_e calculated from eq. (5) depends on the value of regime parameter to be taken, that is, corresponding to regime I and II, respectively.

To determine the operating regime, one can make use of the approximate form Lauritzen Z-test:[46]

$$Z \approx 10^3 (L/2a)^2 \exp(-X/T_c \Delta T), \qquad (12)$$

where Z is a dimensionless parameter. For regime I, $Z \leq 0.01$ and for regime II, $Z \geq 1$. L is the effective substrate length, and 'a' is the molecular chain width. The parameter $X = K_g$ for regime I and $X = 2K_g$ for regime II.

Using the values of K_g, from Table V, the estimated values of L using T^0_{mLHW} are displayed in Table VI. The maximum values of L obtained for regime I are either lesser than or just slightly more than the molecular chain width. As the critical nucleus tends to in the range of few molecular widths, this seems an unreasonable value. The results effectively rule out regime I as a probable operating regime.

Runt et al.[47] on applying the Lauritzen Z-test on the growth rate data of Van Antwerpen and Van Krevelen[1] calculated the values of L ranged from few tens of angstrom at the lowest T_c to few thousand at the highest T_c This had corresponded to regime II growth for the temperature range 120–200°C. No regime transition was reported for that range of temperatures. In the present case, the calculated minimum values of L, values for regime II kinetics range from few thousand to a few tens of thousands angstrom. Runt et al. point out that the guidelines as to what would constitute a reasonable value of the substrate length are not well defined. However, the authors, for polybutylene terephthalate (PBT), estimated the minimum value of L at the highest T_c to be >390 Å. This was in close proximity to the value reported for polyethylene. Furthermore, according to Palys and Philips[21] the lamellar width observed from electron micrographs for PET never exceeds 1000 Å and remained closer to 500 Å. The results, in this context, especially for lower concentrations and higher temperatures appear to be on the higher side for regime II kinetics.

The maximum values of L, for regime I, calculated using the values of T^0_{mNLHW} is in the range of few hundred angstroms, which appears a more reasonable estimate. The values are displayed in Table VII. These results seem to suggest regime I to be the operating regime for all concentrations. The minimum values of L, obtained for regime II were extremely high, ruling it out a probable operating regime.

The calculated values L, in both cases are sensitive to temperature, increasing with the temperature due to a corresponding decrease in surface nucleation rate (i). The addition of the nucleating agent has also resulted decrease in substrate length especially for higher concentrations of the agent.

Thus, applying Z-test using T^0_{mNLHW} and T^0_{mLHW}, yields different conclusions as to the probable operating regime. To account for the discrepancy, further

TABLE VI
Substrate Length Calculated using T^0_{mLHW}

		Regime I (Å)	Regime II (Å)
Sample	Temperature (°C)	$X = K_g$, $Z = 0.01$	$X = 2K_g$, $Z = 1$
Pure PET	195	3.01	3125.79
	200	3.91	5283.01
	205	5.28	9659.90
	210	7.50	19,464.24
	215	11.32	44,300.25
	220	18.45	117,815.56
1% SA	200	2.86	2830.37
	205	3.82	5060.52
	210	5.36	9957.75
	215	7.99	22,112.18
	220	12.88	57,368.81
	225	22.98	182,708.41
3% SA	205	2.14	1579.04
	210	2.91	2931.65
	215	4.20	6102.19
	220	6.53	14,734.27
	225	11.19	43,353.30
	230	21.99	167,338.56
5% SA	210	1.61	896.87
	215	2.21	1694.70
	220	3.24	3640.86
	225	5.18	9278.27
	230	9.29	29,882.12
10% SA	210	1.72	1021.38
	215	2.40	1985.57
	220	3.58	4429.63
	225	5.86	11,884.25
	230	10.91	41,159.33

TABLE VII
Substrate Length Calculated from T^0_{mNLHW}

Sample	Temperature (°C)	Regime I (Å) $X = K_g$, $Z = 0.01$	Regime II (m) $X = 2K_g$, $Z = 1$
Pure PET	195	547.99	1.04×10^{-2}
	200	747.68	1.93×10^{-2}
	205	1051.19	3.82×10^{-2}
	210	1529.18	8.09×10^{-2}
	215	2313.04	1.85×10^{-1}
	220	3659.56	4.63×10^{-1}
1% SA	200	348.71	4.21×10^{-3}
	205	492.54	8.39×10^{-3}
	210	721.81	1.80×10^{-2}
	215	1103.83	4.22×10^{-2}
	220	1773.92	1.09×10^{-1}
	225	3022.08	3.16×10^{-1}
3% SA	205	174.28	1.05×10^{-3}
	210	252.87	2.21×10^{-3}
	215	383.52	5.09×10^{-3}
	220	612.84	1.30×10^{-2}
	225	1042.07	3.76×10^{-2}
	230	1909.59	1.26×10^{-1}
5% SA	210	82.92	2.38×10^{-4}
	215	119.92	4.98×10^{-4}
	220	181.70	1.14×10^{-3}
	225	291.06	2.93×10^{-3}
	230	498.55	8.60×10^{-3}
10% SA	210	98.74	3.37×10^{-4}
	215	145.56	7.33×10^{-4}
	220	225.61	1.76×10^{-3}
	225	371.33	4.77×10^{-3}
	230	657.35	1.49×10^{-2}

investigation was carried out using the exact form of the *Z*-test:[48]

$$Z = (L/2a)^2 \left[\exp\left(\frac{2ab\sigma_e(1+\Phi)}{k_B T_c}\right)\right]\left[\exp\left(-\frac{X}{T_c \Delta T}\right)\right]. \quad (13)$$

In eq. (12), the first exponential term in eq. (13) has been approximated to 10^3.The fold surface energy assuming regime I and II was calculated by taking $m = 4$ and 2, respectively. The term $(1 + \Phi)$ is absent for regime I. For regime II, Φ can values ranging from one to zero. In regime II, $\Phi = 0$ corresponds to total adsorption of polymer chain prior to attachment as surface nucleus. $\Phi = 1$ corresponds to a situation where the polymer chain directly travels from the melt and deposits as a nucleus without any transitory phase. All the other parameters in the equation have been defined previously. The calculated minimum values of L for regime I and maximum values of L in regime II (for pre-adsorption and direct deposition mode) are shown in Table VIII. The calculated maximum values of regime I for the samples mostly range from few angstroms at lower temperature to tens of angstroms at higher temperatures, which is small for regime I. The greater values obtained at higher temperatures may be interpreted as onset of regime I growth. The calculated values from regime II in the pre-adsorption were greater than that obtained for direct deposition mode. $\Phi = 0$ and $\Phi = 1$ represent two extremes, most polymer systems have Φ values in between zero and one with the pre-adsorption mode being more favored.[20] It is also interesting to note that, for regime II, reasonable values of L can be obtained in between that observed for the two modes.

Table IX lists the substrate lengths calculated using T^0_{mNLHW} and the exact from of Z. The calculated values of L for regime I are too low for it to be considered a probable operating regime. For regime II, while in the pre-adsorption mode slightly high values were obtained, for $\Phi = 1$ extremely low values were obtained. The difference in the L values obtained from the exact form and the approximate form of the *Z*-test can largely be attributed to the procedure of approximating the first exponential term in eq. (13) to 10^3.

Thus, the results of *Z*-test indicate regime II as operating regime for all concentrations. However,

TABLE VIII
Substrate Length Calculated Using Exact Equation and T^0_{mLHW}

Sample	Temperature (°C)	Maximum value of L for regime I (Å)	Minimum value of L for regime II (Å) $\Phi = 0$	$\Phi = 1$
Pure PET	195	5.99	392.47	1.56
	200	8.02	703.26	2.96
	205	11.16	1361.62	6.07
	210	16.29	2901.74	13.68
	215	25.25	6976.93	34.75
	220	42.30	19,580.13	102.90
1% SA	200	7.33	588.24	3.87
	205	10.07	1108.50	7.68
	210	14.49	2296.46	16.75
	215	22.14	5363.22	41.14
	220	36.55	14,619.15	117.81
	225	66.83	48,868.20	413.33
3% SA	205	8.00	700.99	9.84
	210	11.15	1360.22	19.96
	215	16.44	2956.43	45.29
	220	26.09	7447.58	119.04
	225	45.69	22,842.53	380.60
	230	91.62	91,832.15	1593.65
5% SA	210	8.04	707.82	17.66
	215	11.27	1389.01	36.00
	220	16.82	3096.75	83.29
	225	27.35	8183.43	228.25
	230	49.96	27,310.66	789.32
10% SA	210	8.65	817.87	20.71
	215	12.28	1650.97	43.41
	220	18.69	3821.62	104.26
	225	31.17	10,630.56	300.70
	230	59.05	38,145.59	1117.94

TABLE IX
Substrate Length Calculated Using Exact Equation and T^0_{mNLHW}

Sample	Temperature (°C)	Maximum value of L for regime I (Å)	Minimum value of L for regime II	
			$\Phi = 0$	$\Phi = 1$
Pure PET	195	1.42	22.12	1.03×10^{-6}
	200	2.06	46.31	2.57×10^{-6}
	205	3.05	101.96	6.75×10^{-6}
	210	4.66	237.90	1.87×10^{-5}
	215	7.36	593.43	5.51×10^{-5}
	220	12.09	1599.90	1.75×10^{-4}
1% SA	200	7.32	586.99	2.59×10^{-4}
	205	11.17	1364.80	7.02×10^{-4}
	210	17.64	3405.11	2.03×10^{-3}
	215	29.03	9222.62	6.38×10^{-3}
	220	50.14	27,504.09	2.20×10^{-2}
	225	91.65	91,909.32	8.45×10^{-2}
3% SA	205	12.02	1581.19	7.52×10^{-3}
	210	18.59	3779.20	2.04×10^{-2}
	215	29.99	9843.44	6.02×10^{-2}
	220	50.94	28,388.23	0.20
	225	91.94	92,480.44	0.72
	230	178.62	349,076.50	3.05
5% SA	210	13.28	1929.88	0.05
	215	20.28	4498.33	0.13
	220	32.40	11,484.22	0.37
	225	54.67	32,696.13	1.15
	230	98.53	106,219.60	4.15
10% SA	210	15.57	2652.94	0.07
	215	24.24	6426.45	0.18
	220	39.62	17,172.27	0.53
	225	68.70	51,634.53	1.77
	230	127.99	179,225.00	6.79

from isothermal temperature 215°C onward the results do point to a gradual change towards regime I growth. Furthermore, considering $\Phi = 0$ the lower values of substrate length obtained in the nucleated PET (usingT^0_{mLHW}) indicate a shift of the regime I to regime II transition to higher temperatures. This may also interpreted as the growth being more spherulitic in nature.

To further test the applicability of the T^0_m obtained from the nonlinear method, a comparison of the values obtained for l^* (calculated using T^0_{mNLHW}) with the values of l reported by Groeninckx et al.,[49] was carried out. The initial lamellar thickness was calculated using the following procedure. The fold surface energy assuming regime II ($m = 2$) was used to calculate C_2 using eq. (8) and the values of a listed in Table IV. C_2 was further substituted in eq. (8) to obtain the initial lamellar thickness l^*. In the calculations, T^0_m was taken in degrees and ΔH_f was assumed to be 2.1×10^8 J/m^3. The values of l^* are displayed in Figure 9. In general, the initial lamellar thickness decreased with SA concentration. In addition, as expected, it increased with crystallization temperature. The calculated values of l^*, for pure

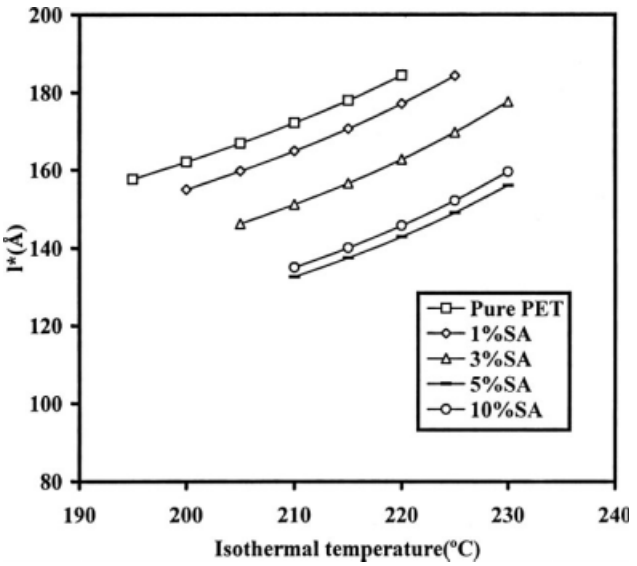

Figure 9 Plot of initial lamellar thickness (l^*) with temperature for pure and nucleated PET.

PET, in the range of temperatures currently studied, are in the range of 150–180 Å. These are much higher than the values l reported to be between 50 and 70 Å (using small angle X-ray scattering). The authors had reported the lamellar thickness of PET crystallized in a similar temperature range (200–225°C) and to a similar degree of crystallinity (41–47%) as the current study. The lamellar thickness calculated assuming regime I were lower in the range of 80–90 Å. This value is still high considering the lamellae thicken during isothermal crystallization. A similar overestimation of was obtained for syndotactic polypropylene by Supaphol et al.[40]

Thus, T^0_m calculated from the NHLW procedure seems inapplicable in the current study. The fold surface energy of the samples calculated using T^0_{mLHW} and $m = 2$corresponding to regime II are displayed in Table X. The fold surface energy is linked to work of chain folding (q), that is, the work done in folding the polymer chain back on to itself. It can be obtained from the relation[20,21,47]:

$$\sigma_e \approx \sigma_+ q/2ab, \tag{14}$$

TABLE X
Fold Surface Energy (σ_e) and Work of Chain Folding (q) of Samples Calculated Using T^0_{mLHW}

Sample	σ_e (J/m^2)	q (joules)
Pure PET	0.133	6.13×10^{-20}
1% SA	0.122	5.58×10^{-20}
3% SA	0.105	4.70×10^{-20}
5% SA	0.092	4.03×10^{-20}
10% SA	0.091	4.01×10^{-20}

where *ab* is the cross-sectional area.[21] The calculated values are shown in Table X. Both q and σ_e decrease with the addition of nucleating agent indicating that the crystallization process should get easier. We had previously reported[16] that chemical nucleation mechanism of SA had caused a reduction in intrinsic viscosity as a result of decrease in molecular weight. The resulting enhanced mobility would have contributed to the reduction in q and σ_e. It also should be noted that at higher concentrations of SA. q and σ_e shows limited variation with SA. Thus, it appears that the unreacted SA might be posing a hindrance to the chain folding process, at those concentrations.

CONCLUSIONS

The nucleating agent has succeeded in promoting greater rate of crystallization in PET. The growth of initially formed nucleus is mainly governed by regime II kinetics in the range of temperatures studied. The measurement of equilibrium melting temperature through the nonlinear Hoffman Weeks method seems to yield an overestimation of T_m^0 and hence is inapplicable in the current study. The addition of SA has also resulted in decrease in q and σ_e. At a given under cooling, the fold surface energy plays major role in the development of the initial lamellar thickness [eq. (7)]. A decrease in σ_e would be seen to promote thinner initial lamellae in PET, which grow at a faster rate resulting in the increase in the overall spherulite growth rate. At lower concentrations up to 3% SA, the combined effect of increase in the primary nucleation rates as well as easing of the growth of the primary nuclei through surface nucleation and chain folding has resulted in k showing a consistent increase with SA concentration. At higher concentrations (5%, 10%) the unreacted SA might be hindering the chain folding process. However, an increase in the primary nucleation rates has appeared to nullify any such hindrance to the growth process leading to a continuous increase of k with SA concentration. The high values of the Avrami exponent at lower concentrations of SA might be the result of the precipitated sodium terephthalate chain ends promoting sporadic formation of nuclei especially at higher temperatures This argument may further be supported by the fact the Hoffman analysis indicated no distinct operating regime change at those concentrations A regime shift could have been a contributing factor to the high exponent value through a change in the morphological component in the Avrami exponent. A study of the melting behavior has revealed that the agents promoted the formation of thinner mature lamellae in PET. The thinner initially formed lamellae in the nucleated samples tended to undergo greater thickening, during isothermal crystallization as compared to pure PET. Thinner mature lamellae combined with a decrease in substrate length, especially for higher concentrations of SA (seen from the Lauritzen *Z*-test), would result in the spherulites attaining a finer texture for those samples.

The authors thank Prof. A. K. Kalkar (Department of Physics, ICT) for his invaluable inputs during the compilation of the article. We would like to extend our gratitude towards them in this regard.

References

1. Van Antwerpen, F.; Van Krevelen, D. W. J Polym Sci Polym Phys Ed 1972, 10, 2423.
2. Turturro, G.; Brown, G. R.; St-Pierre, L. E. Polymer 1984, 25, 659.
3. Przygocki, W.; Wlochowicz, A. J Appl Polym Sci 1975, 19, 2683.
4. Aharoni, S. M. J Appl Polym Sci 1984, 29, 853.
5. Martinez-Vazquez, D. G.; Medellin-Rodriguez, F. J.; Phillips, P. J.; Sanchez-Valdes, S. J Appl Polym Sci 2003, 88, 360.
6. Kim, H. C.; Lee, H.; Kim, H. Y.; Pak, P. K.; Lee, B. O. Polym-Korea 1999, 23, 25.
7. Chen, Y.; Xu, M.; Li, Y.; He, J. Acta Polym Sin 1999, 1, 13.
8. Ye, M.; Wang, X.; Huang, W.; Hu, J.; Bu, H. J Therm Anal 1996, 46, 905.
9. Bian, J.; Sheng-Rong, Y.; Lin-Xian, F. J Polym Sci B Polym Phys 2003, 41, 2135.
10. Jiang, X. L.; Luo, S. J.; Sun, K; Chen, X. D. Express Polymer Lett 2007, 1, 245.
11. Legras, R.; Mercier, J. P.; Nield, E. Nature 1983, 304, 432.
12. Garcia, D. J Polym Sci Polym Phys Ed 1984, 22, 2063.
13. Legras, R.; Bailly, C.; Daumerie, M.; Dekoninck, J. M.; Mercier, J. P.; Zichy, V.; Nield, E. Polymer 1984, 25, 835.
14. Legras, R.; Dekoninck, J. M.; Vanzieleghem, A; Mercier, J. P.; Nield, E. Polymer 1986, 27, 109.
15. Dekoninck, J. M.; Legras, R.; Mercier, J. P. Polymer 1989, 30, 910.
16. Deshpande, V. D.; Jape, S. J Appl Polym Sci 2009, 111, 1318.
17. Avrami, M. J Chem Phys 1939, 7, 1103.
18. Avrami, M. J Chem Phys 1940, 8, 212.
19. Avrami, M. J Chem Phys 1941, 9, 177.
20. Hoffman, J. D.; Davis, G. T.; Lauritzen, J. I. In Treatise on Solid State Chemistry; Hannay, N. B., Ed.; Plenum Press: New York, 1976; Vol.3, Chapter 7, p 497.
21. Palys, L. H.; Philips, P. J. J Polym Sci 1980, 18, 829.
22. Liu, X. F.; Hay, J. N. Polymer 2001, 42, 9423.
23. Balamurugan, G. P.; Maiti, S. N. J Appl Polym Sci 2008, 107, 2414.
24. Chisholm, B.; J; Zimmer, J. G. J Appl Polym Sci 2000, 76, 1296.
25. Binsbergen, F..L. J Polym Sci Polym Symp 1977, 59, 11.
26. Lorenzo, A. T.; Arnal, M. L.; Albuerne, J.; Müller, A. J. Polym Test 2007, 26, 222.
27. Vilanova, P. C.; Ribas, S. M.; Guzman, G. M. Polymer 1985, 26, 423.
28. Kong, Y.; Hay, J. N. Polymer 2003, 44, 623.
29. Wang, Z. G.; Hsiao, B. S.; Sauer, B. B.; Kampert, W. G. Polymer 1999, 40, 4615.
30. Medellin-Rodriguez, F.; J; Phillips, P. J.; Lin, J. S.; Campos, R. J Polym Sci B Polym Phys 1997, 35, 1757.
31. Tiganis, B. E.; Shanks, R. A.; Long, Y. J Appl Polym Sci 1996, 59, 663.
32. Gilmer, J. W.; Neu, R. P.; Liu, Y. J.; Jen, A. K.-Y. Polym Eng Sci 1995, 35, 1407.

33. Hoffman, J. D.; Weeks, J. J. J Res Nat Bur Stand 1962, 66A, 13.
34. Reinsch, V. E.; Rebenfeld, L. J Appl Polym Sci 1994, 52, 649.
35. Marand, H.; Xu, J.; Srinivas, S. Macromolecules 1998, 31, 8219.
36. Lauritzen, J. I.; Passaglia, E. J Res Nat Bur Stand 1960, A64, 73.
37. Dangseeyun, N.; Srimoaon, P.; Supaphol, P.; Nithitanakul, M. Thermochimica Acta 2004, 409, 63.
38. Juhász, P.; Varga, J.; Belina, K.; Marand, H. J Therm Anal Calorim 2002, 69, 561.
39. Wu, P.-L.; Woo, E. M. J Polym Sci B Polym Phys 2002, 40, 1571.
40. Supaphol, P.; Spruiel, J. E.; Lin, J.-S. Polym Int 2000, 49, 1473.
41. Jiannong, X.; Srivatsan, S.; Marand, H. Macromolecules 1998, 31, 8230.
42. Zhang, R.-C.; Lu, A.; Xu, Y.; Min, M.; Xia, J.-Q.; Zhou, J.-H.; Huang, Y.-G.; Li, Z.-M. Eur Polym J 2009, 45, 2872.
43. Chan, T. W.; Isayev, A. I., Polym Eng Sci 1994, 34, 461.
44. Rahman, M. H.; Nandi, A. K. Polymer 2002, 43, 6863.
45. Phillips, P. J., Tseng, H. T. Macromolecules 1989, 22, 1649.
46. Lauritzen, J. I. J Appl Phys 1973, 44, 4353.
47. Runt, J; Miley, D. M.; Zhang, X.; Gallagher, K. P.; McFeaters, K.; Fisburn, J Macromol 1992, 25, 1929.
48. Lauritzen, J. I.; Hoffman J. D. J Appl Phys 1973, 44, 10.
49. Groeninckx, G.; Reynaers, H.; Berghmans, H.; Smets, G. J Polym Sci Polym Phys Ed 1980, 18, 1311.